Numerical analysis of liquefaction mechanism in hydraulic fill dams

Mahya Hatambeigi & Amir Hamidi
Department of Civil Engineering – Kharazmi University, Tehran, Iran

GEOQuébec 2015
Challenges from North to South
Des défis du Nord au Sud

ABSTRACT
As one of the most complex and controversial topics in geotechnical engineering, liquefaction is a major seismic hazard to various earth structures. Loose and saturated sandy deposits in seismic areas are most susceptible to this phenomenon. Reports of failure in Hydraulic fill dams indicate that one of the most prevalent and destructive failure modes in such geotechnical structures is liquefaction. In this paper, using FDM, the behavior of the Lower San Fernando dam during 1971 earthquake was studied and the corresponding liquefaction induced slide was investigated. So, using nonlinear soil constitutive models, the excessive pore water pressures and displacements in different points of the model were computed. Furthermore, the results were compared with those obtained from field investigations and numerical analyses conducted by other researchers. Based on the current comparisons, the predicted displacements, pore pressures and deformation patterns are in a reasonable agreement with the findings of previous studies.

RÉSUMÉ
La liquéfaction, en tant qu'un des sujets les plus complexes et controversés de la géotechnique, est un aléa sismique majeur pour plusieurs structures de sol. Les dépôts sableux saturés ou à faible densité situés dans les zones sismiques sont les plus susceptibles à ce phénomène. Les cas de rupture de barrages hydrauliques en remblais indiquent qu'un des modes de rupture les plus courants et destructeurs pour de telles structures géotechniques est la liquéfaction. Dans cet article, en utilisant la méthode FDM, le comportement du barrage de San Fernando durant le séisme de 1971, ainsi que le glissement de terrain induit par la liquéfaction correspondant à cet événement ont été étudiés. Pour ce faire, en utilisant les modèles constitutifs non-linéaires du sol, les excès de pressions interstitielles, ainsi que les déplacements à différents points du modèle ont été calculés. De plus, les résultats ont été comparés avec ceux obtenus à partir d'analyses numériques et d'investigations de terrain réalisées par d'autres chercheurs. Basés sur les comparaisons actuelles, les déplacements prévus, les pressions interstitielles et les modes de déformation sont en accord raisonnable avec les résultats d'études antérieures.

1 INTRODUCTION

Hydraulic fill is one of the most cost effective methods of constructing earth fill dams in which the materials are conveyed into their final position in the dam by suspension in flowing water. This method was widely applied during the early 20th century in construction of dams with different purposes like water supply and/or retention of industrial byproducts such as mine tailings (tailings dams). however, the failure of Calaveras dam in 1918, Fort Peck dam in 1938 and the near catastrophic flow slide of Lower San Fernando dam during 1971 earthquake brought the efficiency of hydraulic fill dams under suspicion. Nevertheless, considering the economic benefits resulted from hydraulic fill method, some of the small earth dams and most of tailings dams are still constructed by this method. Moreover, application of the hydraulic fill in tailing dams is continuously promoting and wide investigations have been conducted in this field.

Generally, reported failures of Hydraulic fill dams indicate that liquefaction is one of the most common and destructive modes of failure in such geotechnical structures. This is justifiable based on the loose and saturated layers of uniform soil by which hydraulic fill dams are constructed. Unfortunately, eyewitness detailed account regarding the triggering of failure is missing from most of the cases surveyed; in only one case, the Lower San Fernando Dam, adequate geotechnical field works have been available for further study. The flow failure of the upstream slope of this hydraulic fill dam during the 1971 San Fernando Earthquake with magnitude of 6.6 represents the best documented case history of seismically induced liquefaction flow failure of an earth structure.

In the current study, making use of Finite Difference Method, the liquefaction mechanism occurred in Lower San Fernando dam during 1971 earthquake has been investigated. Furthermore, the resulted excessive pore water pressures and soil displacements in different points of the corresponding dam are presented in the analysis. Moreover, the results are compared with those obtained from field investigations by seed et al. (1973) and numerical analyses conducted by Khoei et al. (2004).

2 THE FAILURE OF LOWER SAN FERNANDO DAM

Located in Northern San Fernando Valley, the Los Angeles dam, along with hydraulic fill Lower and Upper San Fernando dams form the Van Norman hydraulic complex, which is critical to the Los Angeles area and controls about 50 to 75 percent of the cities' total water supply (Mayoral and Romo, 2008).

The 1971 San Fernando earthquake triggered severe longitudinal cracks running almost the entire length of the Upper San Fernando dam. These cracks were a product of the dam moving downstream about 1.5 meters and settling about one meter (Seed et al., 1973). On the other

hand, the Lower San Fernando dam experienced a major flow slide which caused most of the upstream shell to slide into the reservoir. The failure of the Lower San Fernando dam was the most serious effect of this earthquake, which has been studied by numerous researches and practitioners in the past. Figure 1 illustrates typical cross sections of the Lower San Fernando dam before and after the slide.

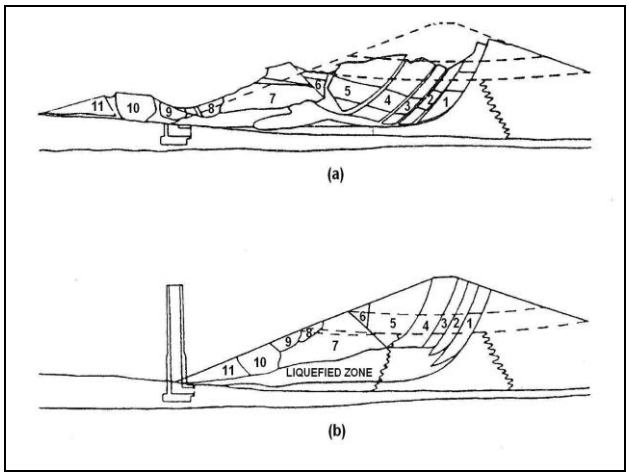

Figure 1. Lower San Fernando dam cross sections (a) after earthquake, (b) reconstructed (seed et al. 1973)

As shown in the above figure, the liquefied area was a narrow wedge in the upstream zone of the dam, which has suffered from progressive reduction of strength due to earthquake induced excess pore water pressures. When the liquefied hydraulic fill material flowed out, it carried the overlying layers broken into intact blocks riding over it. The failure slide appears to have retained sufficient strength to have moved as intact blocks, while the liquefied soil has infiltrated between the large chunks of soil and disappeared into the reservoir bottom. Once the blocks are put together like pieces of a puzzle, the original dam cross section is appeared.

3 THE NUMERICAL MODEL

In order to simulate the discussed failure mechanism of Lower San Fernando dam, a numerical analysis is carried out making use of Finite Difference Method. The idealized geometry of the dam and the finite difference mesh used in the static and dynamic analyses are shown in Figures 2 and 3, respectively.

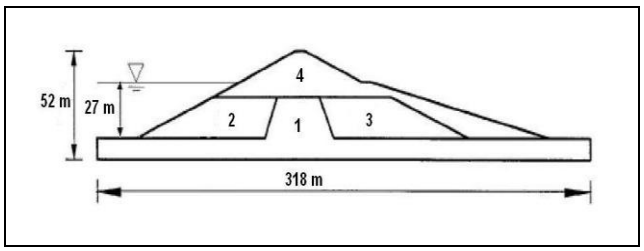

Figure 2. Geometry and material zones of Lower San Fernando dam

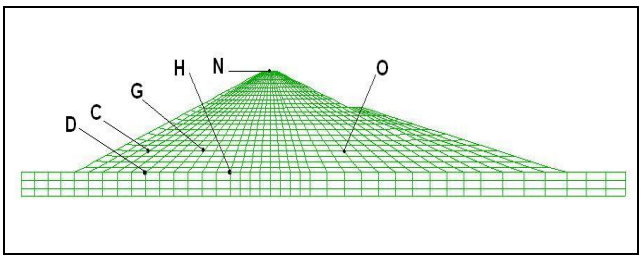

Figure 3. Finite Difference Mesh used for the analysis

The dam was located on a 10 meters alluvial layer consisted of stiff clay and lenses of sand/gravel. It was constructed using variations of the hydraulic fill method that had yielded a central clayey core in the zone 1 and coarse grained shells consisted of sand and silty sand in zones 2 and 3. The rolled fill material of zone 4 was added later up to the height of 42 meters to increase the reservoir capacity.

General properties of the material, along with the parameters of Mohr-Coulomb model used in the lower San Fernando dam analysis are listed in Table 1 for different zones of the dam.

Table 1. Material properties in different zones of the Lower San Fernando dam (Khoei at al. 2004)

Zone	1	2	3	4
Dry density (Kg/m^3)	1722	1652	1652	1652
Saturated density	2090	2020	2020	2020
Modulus of Elasticity (MPa)	153	89.3	96	106
Poisson's ratio	0.3	0.3	0.3	0.3
Effective internal friction angle (deg.)	0	37	37	37
Effective cohesion (kPa)	96	0	0	0
Porosity	0.4	0.4	0.4	0.4
Normalized standard penetration test value	-	11	12	-

3.1 Soil Constitutive Models

Modeling of the stress−strain behavior of the zones 1 and 4 was carried out simulating the soil as an elasto-plastic material with Mohr-Coulomb criterion and a non-associated flow rule. This constitutive model is the conventional model commonly used to represent stress−strain behavior and the corresponding shear failure in soils and rocks. In addition, simulation of loose and saturated hydraulic fill behavior in upstream shell was made considering Finn model (Martin et al., 1975; Byrne ,1991). Using this constitutive model, the dynamic pore pressure generation, especially, related to the liquefaction can be modeled by accounting for irreversible volume strains. The model captures basic mechanisms that can lead to liquefaction in saturated sandy soils.

3.1.1 The principles of Finn Model

Basically, granular materials exhibit permanent volumetric deformation during drained cyclic loading. This permanent volumetric deformation is the primary reason for the progressive build-up of excess pore pressure during undrained cyclic loading that leads to liquefaction. Several empirical formulas have been proposed to compute the volumetric strains due to shear strain changes. Martin et al. (1975) proposed an empirical relationship that relates the incremental volumetric strain, $\Delta\varepsilon_{vd}$, to cyclic shear strain amplitude, γ, (Eq. 1). In this equation, γ is presumed to be the engineering shear strain, ε_{vd} is the current accumulated volumetric strain and C_1, C_2, C_3, and C_4 are constants.

$$\Delta\varepsilon_{vd} = C_1\left(\gamma - C_2\varepsilon_{vd}\right) + \frac{C_3\varepsilon_{vd}^2}{\gamma + C_4\varepsilon_{vd}} \qquad [1]$$

It must be noted that the above equation enables the volumetric strain increment to decrease with accumulation of strain. Another alternative and simple formula that was used in this work (Eq. 2) is proposed by Byrne (1991):

$$\frac{\Delta\varepsilon_{vd}}{\gamma} = C_1 \exp\left(-C_2\left(\frac{\varepsilon_{vd}}{\gamma}\right)\right) \qquad [2]$$

where C_1 and C_2 are constants with different interpretations from those of Eq. 1, and can be related to the relative density, D_r, and the normalized standard penetration test value, $(N_1)_{60}$, by the following equations:

$$C_1 = 7600\left(Dr\right)^{-2.5} \qquad [3]$$

$$Dr = 15\left(N_1\right)_{60}^{0.5} \qquad [4]$$

Finn model incorporates Eq. 2 into the standard Mohr-Coulomb plasticity model to simulate the mechanism that can lead to liquefaction.

4 STATIC ANALYSIS

The distribution of pore pressures and vertical stresses in the dam body at steady state condition is computed at this stage. In this regard, the dam body was subjected to self weight and analyzed statically. The results of static analysis are shown in Figure 4 as total stresses, vertical effective stresses and pore pressure contours at the steady state condition.

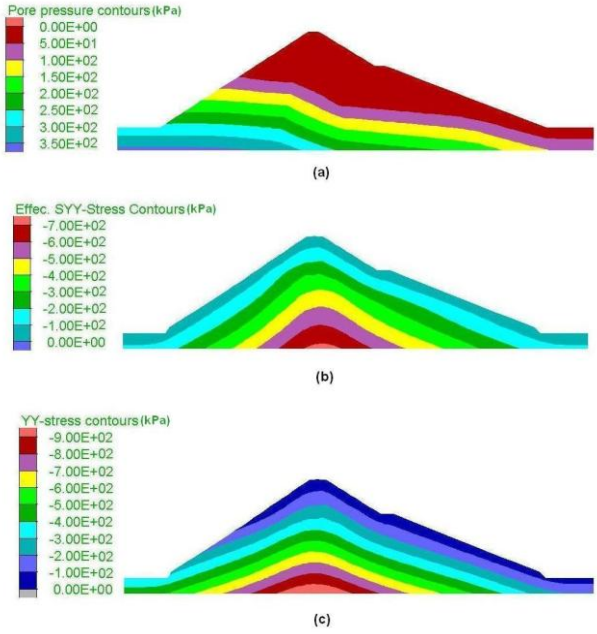

Figure 4. The distribution of (a) pore pressure, (b) effective vertical stress, (c) total vertical stress, at steady state condition

5 DYNAMIC ANALYSIS

Numerical methods relying on the discretization of a finite region of space require the appropriate conditions enforced at the artificial numerical boundaries. In static analyses, fixed or elastic boundaries can be realistically placed at some distance from the region of interest. However, in dynamic problems such boundary conditions cause the reflection of upward propagating waves back into the model and do not allow the necessary energy radiation. So, instead of simple boundary conditions used in static analyses, the free-field boundary conditions were applied to the left and right sides of the model boundaries.

Several time histories were recorded at locations surrounding the Lower San Fernando dam during 1971 earthquake. Just as past studies of the dam's failure, the time history recorded on the abutment of Pacoima dam located about 5 km east of San Fernando dam is used in the current study. Past studies had estimated the base rock peak ground acceleration (PGA) of 0.6g at the dam site. So, the PGA of the Pacoima record is scaled to 0.6g and applied directly at the bottom boundary of the numerical model. As shown in Figure 5, the modified time history includes about 12 seconds of the strong motion. Figure 6 shows the pore pressure contours after 15 seconds of the earthquake. Significant amounts of pore pressure developed after the earthquake in the upstream and downstream hydraulic fill shells implicates that an extensive liquefaction has happened in these parts of the dam body.

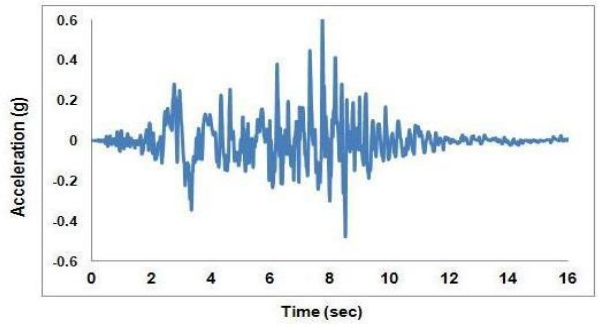

Figure 5. Scaled Pacoima dam record of 1971 San Fernando earthquake

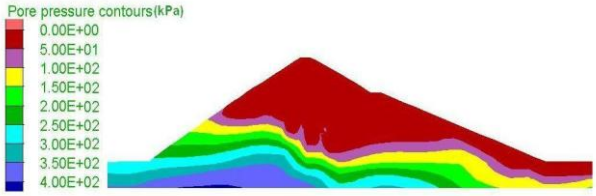

Figure 6. Pore pressure distribution after 15 seconds of earthquake loading

Moreover, referring to Figures 7 and 8 that respectively show the displacement contours and vectors of the dam body after 15 seconds into the earthquake, it is evident that a large slide has begun in the upstream slope of the dam, compared to which, the downstream slope has moved very little. It should be mentioned that the pattern of failure observed here is in a good agreement with that presented by Seed at al. in Figure 1.

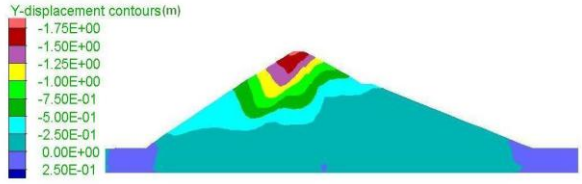

Figure 7. Vertical displacements of the dam after 15 seconds of earthquake loading

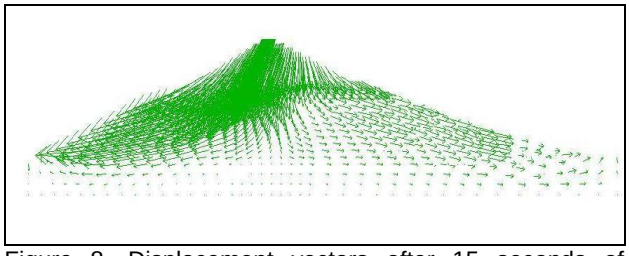

Figure 8. Displacement vectors after 15 seconds of earthquake loading

The variation of excess pore water pressure versus time at different nodes, as specified in Figure 1, are shown in Figure 9. The larger values of excess pore water pressure at the nodes near the upstream slope in the center portion of the dam, i.e. nodes G and H, is conspicuously observed. Figure 10 illustrates the variation of horizontal and vertical displacements during the earthquake at nodes G and O located on the same elevation, yet different sides of the clayey core of the dam. A comparison between the displacement magnitude of nodes G and O confirms that the upstream slope has undergone much higher values of deformation compared to the downstream side of the dam, thus has caused the failure in upstream shell of the dam. The variation of horizontal and vertical displacements at the crest of the dam, node N, are illustrated in Figure 11. As seen, the dam crest has settled about 1.75 meters, which is the maximum value of vertical displacement in the whole dam body.

6 THE COMPARATIVE ANALYSIS OF POST-LIQUEFACTION PROCESS

At the end of the earthquake, the pore pressure values in upstream shell region are considerably increased and the soil situated in this zone is completely liquefied. In this occasion, with initiation of sandy soil consolidation and excess pore water pressure dissipation, the latter stage starts just at the end of applying the earthquake loading. This stage is characterized by decreasing the residual pore pressure with time as discussed by Kudella and Oumeraci (2004).

In this part of the study, in order to investigate the post-liquefaction conditions as well as evaluating the accuracy of the analysis, a comparison is made between the results of the current numerical study and the one by Khoei et al. (2004) which is conducted using Pastor–Zienkiewicz and Cap plasticity models. In this regard, the variation of excess pore water pressures at node H and vertical displacements in node N, dam crest, after 100 seconds are plotted with the results of Khoei et al. (Figures 12 and 13). Based on the comparative figures, it is noted that the maximum value of excess pore pressures generated in node H are almost equal to the peak values concluded from Pastor- Zienkiewicz model, while the Cap model has resulted in higher values. However, Pastor–Zienkiewicz model estimates the peak of excess pore pressure after the end of earthquake, whereas both Finn and Cap evaluate those peaks during the earthquake. Additionally, it is observed in Figure 13 that all three models have led to the same maximum displacement of dam crest after 100 seconds, although the maximum value by Cap and Finn are reached prior to Pastor-Zienkiewicz model. Nevertheless, based on the overall variations of selected nodes, it is logical to conclude that the Finn model has presented a reasonable agreement with Cap and Pastor-Zienkiewcz models.

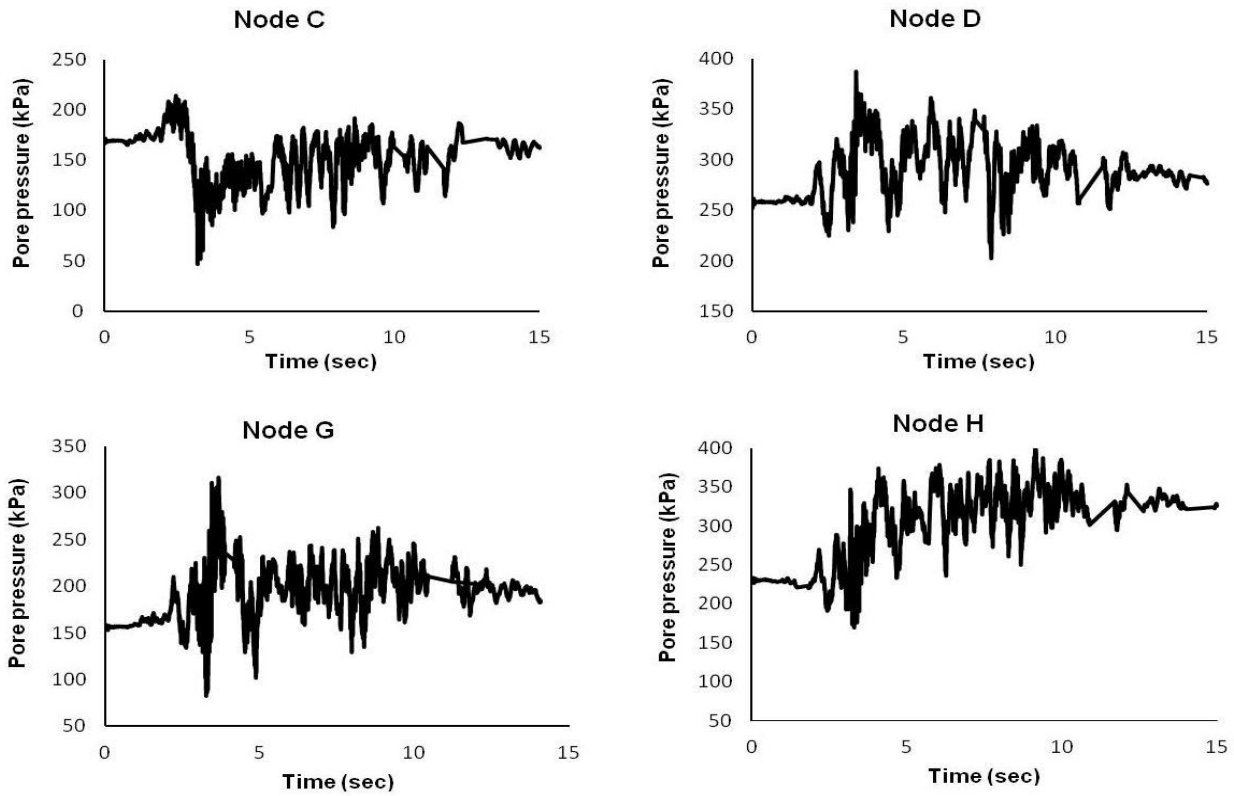

Figure 9. The variation of excess pore water pressure with time at different nodes during earthquake loading

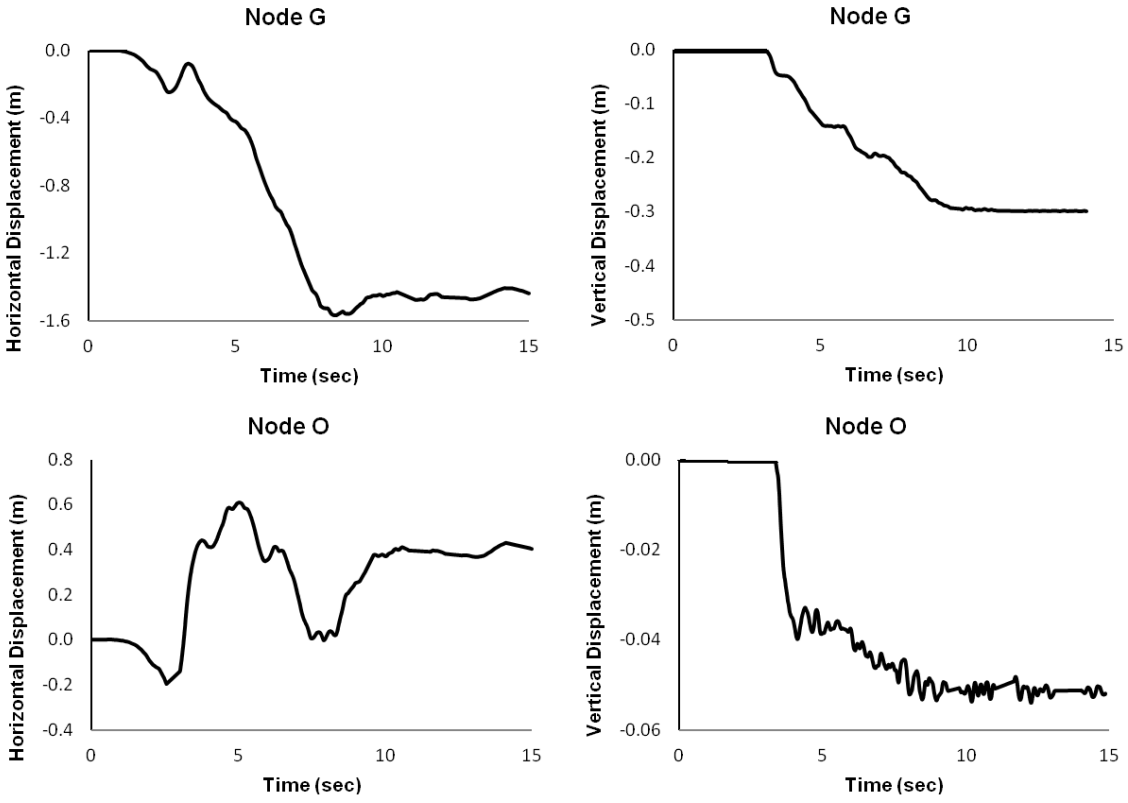

Figure 10. The variation of horizontal and vertical displacements at different nodes during earthquake loading

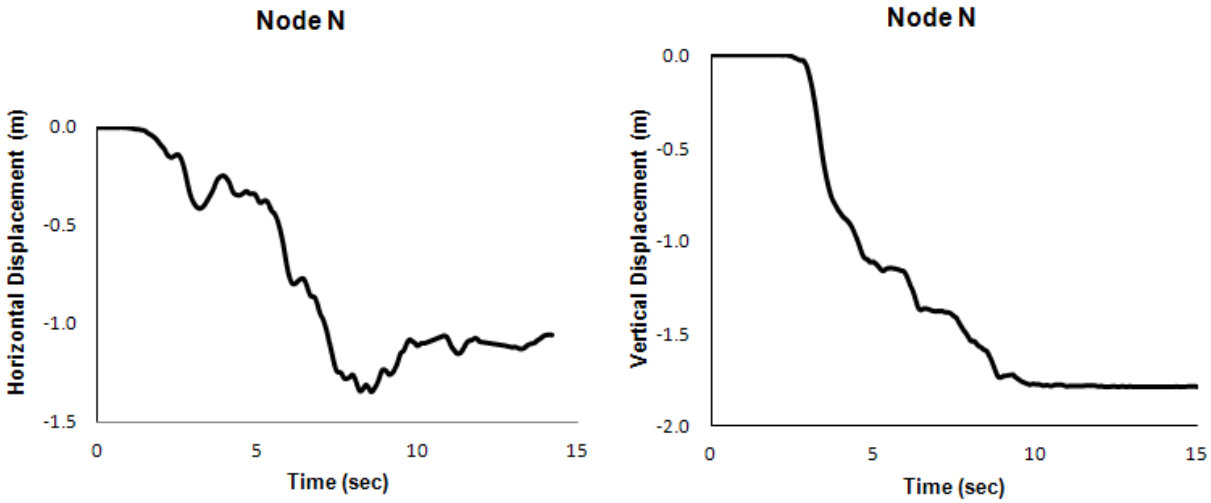

Figure 11. The variation of horizontal and vertical displacements at the dam crest during earthquake loading

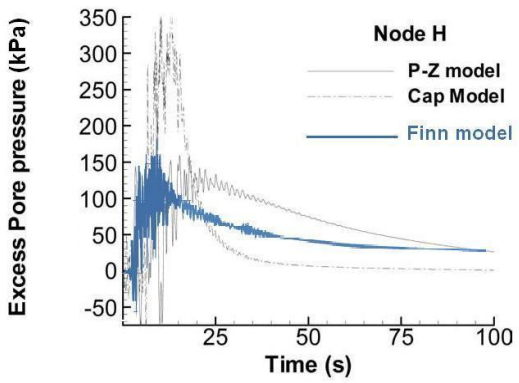

Figure 12. The variation of excess pore pressure at node H using Finn, cap plasticity, and Pastor–Zienkiewics models

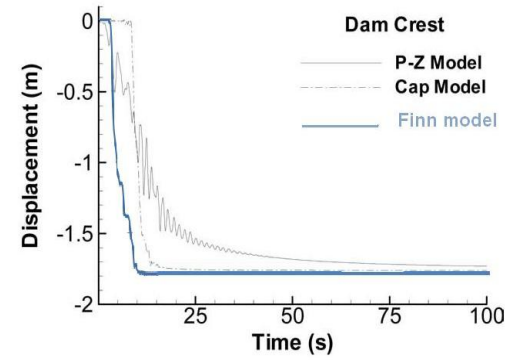

Figure 13. The variation of vertical displacement at dam crest using Finn, cap plasticity, and Pastor–Zienkiewics models

7 CONCLUSIONS

In order to investigate the liquefaction mechanism in hydraulic fill dams, the liquefaction of Lower San Fernando dam during 1971 earthquake, as one the best documented cases of flow failure liquefaction so far, was modeled and the corresponding slide of the upstream slope of the dam was studied. Accordingly, pore water pressure and displacements changes in different parts of the dam were simulated by a Finite Difference Method. Based on the results of dynamic analysis conducted by Finn constitutive model, it is observed that following the significant increase in the pore water pressure of hydraulic fill material situated in upstream slope, a critical liquefied zone has formed in upstream shell. The zone has subsequently flowed out, which has led to the large settlements of overlaying layers and the initiation of the slide in upstream side of the dam. The pattern of failure resulted from the current numerical study was analogous to the one investigated by Seed et al. (1973), which confirms the success of Finn model in simulating the failure mechanism occurred in the Lower San Fernando dam.

Furthermore, in order to investigate the post-liquefaction condition, the behavior of dam was investigated 100 seconds after the earthquake loading and the resultant variations of pore water pressures and displacements with time were plotted. It is shown that the reduction of pore water pressure has a high rate at the beginning and then its rate becomes lower. Hence, quite a long period of time is needed for complete pore pressure dissipation.

Finally, In order to evaluate the accuracy of the current study, the results of this study were compared to another numerical analysis using Pastor-Zienkiewicz and cap plasticity models by Khoei et al. on two selected points of the same dam. Based on the carried out comparison, it is deduced that the results of the Finn model are in a better

agreement with those of Pastor-Zienkiewicz from the peak value point of view. However, it is observed that the time domain in which the peak values of pore pressure and displacement have occurred is almost coinciding through Finn and Cap plasticity models.

REFERENCES

Beaty, M.H. and Byrne, P.M. 2000. A Synthesized Approach for Predicting Liquefaction and Resulting Displacements, *12th World Conference on Earthquake Engineering, Auckland, New Zealand, 1:407-413*

Byrne, P.A. 1991. A cyclic shear-volume coupling and pore-pressure model for sand, *second International Conference on Recent Advances in Geotechnical Earthquake Engineering and Soil Dynamics*, St. Louis, Missouri, USA, 2: 47-44

Byrne, P.M., Park, S.S., Beaty, M., Sharp, M., Gonzalez, L. and Abdoun, T. 2004. Numerical modeling of liquefaction and comparison with centrifuge tests, *Canadian Geotechnical Journal*, 41: 193-211.

Dawson, E.M., Roth, W.H., Nesarajah, S., Bureau, G. and Davis, C.A. 2001. A practice oriented pore pressure generation model, *2nd International FLAC Symposium*, Lyon, France.

Khoei, A.R., Anahid, M., Zarinfar, M., Ashouri, M. and Pak, A. 2011. A Large Plasticity Deformation od Unsaturated Soil for 3D Dynamic Analysis of Lower San-Fernando Dam, *Asian Journal of Civil Engineering (Building and Housing)*, 12(1): 1-25.

Khoei, A.R., Azami, A.R., and Haeri, S.M. 2004. Implementation of plasticity based models in dynamic analysis of earth and rockfill dams: A comparison of Pastor–Zienkiewicz and cap models, *Journal of Computers and Geotechnics*, 31: 385-410.

Khoei, A.R. and Haghighat, E. 2011. Extended finite element modeling of deformable porous media with arbitrary interfaces, *Journal of Applied Mathematical Modelling*, 35: 5426-5441.

Khoei, A.R. and Mohammadnejad, T. 2011. Numerical modeling of multiphase fluid flow in deforming porous media: A comparison between two- and three-phase models for seismic analysis of earth and rockfill dams, *Journal of Computers and Geotechnics*, 38: 142-166.

Martin, G.R., Finn, W.D.L., and Seed, H.B. 1975. Fundamentals of liquefaction under cyclic loading, *Journal of the Geotechnical Engineering, ASCE,* 101(5): 423−438.

Kudella, M. and Oumeraci, H. 2004. *Liquefaction around marine structures (LIMAS)-large scale experiments on a Caisson Breakwater,* Technical University of Braunschweig, Braunschweig, Germany.

Matoral, J.M. and Romo, M.P. 2008. Geo-Seismic Environmental Aspects Affecting Tailings Dams Failures, *American Journal of Environmental Sciences,* 4(3): 212-222.

Mir Mohammad Hosseini, S.M. and Arefpour, B. 1999. *Earthquake Geotechnical Engineering*, International Institute of Earthquake Engineering and Seismology, Tehran, Iran.

Mir Mohammad Hosseini, S.M., Pashang Pisheh, Y., Shakibania, K. and Ganjian, N. 2010. Effect of Density on Critical Depth of Liquefaction in a Soil Deposit Containing Double Loose Sand Lenses, Fifth International Conference on *Recent Advances in Geotechnical Engineering and Soil Dynamics*, San Diego, California, USA.

Pashang Pisheh, Y. and Mir Mohammad Hosseini, S.M. 2010. Numerical simulation of cyclic behavior of double sand lenses and corresponding liquefaction-induced soil settlement, *Journal of Central South University of Technology*, 17: 593-602.

Sadrnejad, S.A. 2011. A multi-lined behavior simulation approach for liquefaction of earth-dam, *Journal of Computational Methods in Civil Engineering*, 2(2): 201-218.

Schuyler, J. D. 1912. *Reservoirs for irrigation, water power and domestic water supply*, John Wiley & Sons, New York, NY, USA.

Seed, H.B., Lee, K.L., Idriss, I.M. and Makdisi, F. 1973. *Analysis of the slides in the San Fernando dams during the earthquake of Feb. 9, 1971. UCB/ERRC-73/02,* Earthquake Engineering Research Center, University of California, Berkeley, USA.

Vafaeian, M. 2005. *Earth Dams*, 4th ed., Isfahan University of Technology, Isfahan, Iran.

Vasquesz-Herra, A. and Dobry, R. 1989. Re-Evaluation of the Lower San fernando dam., U.S. Army Corps of Engineers, Washington, DC, USA.

Vick, S. G. 1983. *Planning, Design, and Analysis of Tailings Dams*, John Wiley & Sons, New York, NY, USA.

Wu, G. 2001. Earthquake-induced deformation analyses of the Upper San Fernando Dam under the 1971 San Fernando Earthquake, *Canadian Geotechnical Journal*, 38: 1-15.

Zienkiewicz, O.C., Chan, A.H.C., Pastor, M., Schrefler, B.A. and Shiomi, T. 1999. *Computational geomechanics with special reference to earthquake engineering*, John Wiley & Sons, New York, NY, USA.